

Geophysical Research Letters®



RESEARCH LETTER

10.1029/2022GL100757

Yuehongjiang Yu and Chuanxi Wang contributed equally to this work.

Key Points:

- Bubbles in subsurface porous media coarsen toward equilibrium, which modifies local thermodynamics, transport, and reactive properties
- Classical *Lifshitz-Slyozov-Wagner* theory fails for bubbles coarsening in porous media, as porous geometry reshapes the concentration profile
- A new theory is derived that predicts the bubble population evolution during coarsening, which helps in modeling complex subsurface flow

Supporting Information:

Supporting Information may be found in the online version of this article.

Correspondence to:

K. Xu,
kexu1989@pku.edu.cn

Citation:

Yu, Y., Wang, C., Liu, J., Mao, S., Mehmani, Y., & Xu, K. (2023). Bubble coarsening kinetics in porous media. *Geophysical Research Letters*, 50, e2022GL100757. <https://doi.org/10.1029/2022GL100757>

Received 6 AUG 2022
Accepted 16 DEC 2022



Author Contributions:

Conceptualization: Ke Xu
Formal analysis: Yuehongjiang Yu, Ke Xu
Funding acquisition: Ke Xu
Investigation: Yuehongjiang Yu, Chuanxi Wang, Ke Xu
Methodology: Ke Xu
Project Administration: Ke Xu
Software: Junning Liu, Sheng Mao, Yashar Mehmani
Supervision: Ke Xu
Visualization: Yuehongjiang Yu, Chuanxi Wang, Junning Liu

© 2022. The Authors.

This is an open access article under the terms of the [Creative Commons Attribution License](https://creativecommons.org/licenses/by/4.0/), which permits use, distribution and reproduction in any medium, provided the original work is properly cited.

Bubble Coarsening Kinetics in Porous Media

Yuehongjiang Yu¹, Chuanxi Wang¹ , Junning Liu², Sheng Mao², Yashar Mehmani³, and Ke Xu^{1,4} 

¹Department of Energy and Resources Engineering, College of Engineering, Peking University, Beijing, China, ²Department of Mechanics and Engineering Sciences, College of Engineering, Peking University, Beijing, China, ³Department of Energy and Mineral Engineering, The Pennsylvania State University, University Park, PA, USA, ⁴Institute of Energy, Peking University, Beijing, China

Abstract Bubbles in subsurface porous media spontaneously coarsen to reduce free energy. Bubble coarsening dramatically changes surface area and pore occupancy, which affect the hydraulic conductivity, mass and heat transfer coefficients, and chemical reactions. Coarsening kinetics in porous media is thus critical in modeling geologic CO₂ sequestration, hydrogen subsurface storage, hydrate reservoir recovery, and other relevant geophysical problems. We show that bubble coarsening kinetics in porous media fundamentally deviates from classical *Lifshitz-Slyozov-Wagner* theory, because porous structure quantizes the space and rescales the mass transfer coefficient. We develop a new coarsening theory that agrees well with numerical simulations. We identify a pseudo-equilibrium time proportional to the cubic of pore size. In a typical CO₂ sequestration scenario, local equilibrium can be achieved in 1s for media consisting of sub-micron pores, while in decades for media consisting of 1 mm pores. This work provides new insights in modeling complex fluid behaviors in subsurface environment.

Plain Language Summary In modeling fluid behaviors during geologic CO₂ sequestration, hydrogen subsurface storage, hydrocarbon recovery and magma kinetics, the evolution of bubbles in subsurface porous media should be resolved to quantify hydraulic conductivity, mass and heat transfer coefficients, and reactional surface area. However, classical *Lifshitz-Slyozov-Wagner* theory qualitatively fails to predict bubbles' coarsening kinetics, as porous structure fundamentally reshapes the mass transfer pattern. A new coarsening theory is derived that perfectly matches numerical simulation. The evolution of free energy, pore occupancy, and surface area can be predicted, and an equilibrium time is identified that determines the validity of the local thermodynamic equilibrium presumption. This work helps to model complex fluid behaviors in many geophysical applications.

1. Introduction

Trapped bubbles are ubiquitous in natural subsurface porous strata. Since they block a portion of the void space and contribute significant fluid–fluid interfacial area, they can have a sizable impact on the hydraulic conductivity (Anton & Hilfer, 1999; Bear, 1996), mass and heat transfer coefficients (Ehlers & Häberle, 2016; Ozgumus & Mobedi, 2015), and chemical reaction rate (Lay et al., 1996; Yortsos & Stubos, 2001) in a porous medium. As a result, the distribution and morphology of a population of bubbles are of significant interest in oil and gas recovery (Gao et al., 2021; Geistlinger et al., 2015; A. Mehmani et al., 2019) and geologic CO₂ storage (Fu et al., 2013; Huppert & Neufeld, 2014; Joewondo et al., 2021; Juanes et al., 2006; Li et al., 2020; Lyu et al., 2021).

After bubbles emerge after direct gas injection, heating, depressurization, or chemical reactions (Danov et al., 2003; Holocher et al., 2003; Lay et al., 1996; Yortsos & Stubos, 2001), they are not immediately at equilibrium, and would spontaneously evolve via ripening to reduce total free energy. Ripening is the process by which bubbles with a high capillary pressure (P_c) dissolve into the wetting phase and transfer their mass, by molecular diffusion, to bubbles with a low P_c . No external forcing is required. An initial distribution of bubbles with different sizes will therefore evolve toward a new distribution that has minimum interfacial free energy (Wang et al., 2021). For example, when bubbles are spherical, capillary pressure follows $P_c = 2\sigma/R$, where σ is the surface tension and R is the radius of the bubble. This means smaller bubbles have a larger capillary pressure. As a result, the ripening of spherical bubbles leads to *coarsening*, a process where small bubbles dissolve and feed into large bubbles. In bulk fluids (Figure 1a), coarsening is unabated and continues until all bubbles merge into one. For an infinitely sparse bubble population, the ripening kinetics are predicted by the *Lifshitz-Slyozov-Wagner* (LSW) theory (Lifshitz & Slyozov, 1961; Voorhees, 1985; Wagner, 1961), which states that the average bubble

Writing – original draft: Yuehongjiang Yu, Chuanxi Wang
Writing – review & editing: Yashar Mehmani, Ke Xu

radius (r_c) scales with time (t) as $r_c^3 \sim t$. Note that the classical LSW theory only deals with ripening in three dimensions. In two dimensions, nevertheless, similar scaling is also derived (Bray, 2002; Rogers & Desai, 1989; Yao et al., 1993). Moreover, each bubble transfers mass with the surrounding mean field (Bray, 2002; Lifshitz & Slyozov, 1961; Yao et al., 1993) as follows:

$$\frac{dV}{dt} = C_{\text{LSW}} R \sigma \left(\frac{1}{R_c} - \frac{1}{R} \right), \quad (1)$$

where $C_{\text{LSW}} = 8\pi\nu c_\infty D/k_B T$ is a constant that contains the atomic volume ν of the solute, the concentration of the saturated solution c_∞ , the diffusivity of the solute in the solution D , the Boltzmann constant k_B , and the temperature T . Equation (1) implies that the driving force is $\sigma(1/R_c - 1/R)$ and the characteristic mass transfer length is R . Note that for a dissolving bubble, the driving force increases while simultaneously the characteristic length decreases.

In a porous medium, however, the bubble size and the mass transfer length are decoupled. Figures 1b and 1c shows the void space can be divided into chambers, or *pores*, connected by converging-diverging segments, or throats. Collectively, these define a graph of admissible diffusion pathways for the dissolved solute. The concentration of the solute in each pore is approximately uniform, because of the larger mass transfer resistance imposed by the surrounding throats (Y. Mehmani et al., 2014). The characteristic length associated with mass transport is therefore dictated by the lattice spacing, L_0 . Due to the decoupling of bubble size from mass transfer length, LSW theory and Equation (1) become invalid for porous-media applications. Simple remedies of correcting the diffusion coefficient, as done by earlier works (Schmelzer et al., 1995; Slezov et al., 1993), fall inadequate. A new theory is required to capture the physics of bubble coarsening in porous media.

In this letter, we aim at (a) numerically demonstrating and rationalizing the failure of LSW theory for bubble coarsening in porous media; (b) theoretically deriving kinetic laws for bubbles coarsening in porous media; and (c) analyzing the time scale for the coarsening in porous media and discussing its implications in geophysical applications.

2. Numerical Simulation in Homogenous Porous Media

We first demonstrate the failure of LSW in porous media by numerical simulations using a recently developed pore-network model (PNM) that has already been validated experimentally (Y. Mehmani & Xu, 2022a, 2022b).

In the PNM, the complex void geometry of a porous medium is replaced by an interconnected network of pores and throats. The PNM is quasi-static, fully implicit, and employs adaptive time stepping. The PNM can model mass transport by diffusion following Fick's law, while no convection is included. The PNM is sufficient to model the ripening process in this paper. The quasi-static hypothesis is rationalized in Supporting Information. The PNM has been validated against published micromodel experiments (K. Xu et al., 2017). The PNM is not limited to the geometrical structure.

We simulate the ripening of 40,000 bubbles inside a 200×200 lattice pore network. Each pore is connected to four neighboring pores through the throats. The pores are cubic in shape for simplicity. The lattice spacing L_0 is $10 \mu\text{m}$, which is equal to the sum of the throat length, L_t ($8 \mu\text{m}$), and the pore-body length, $2L_p$ ($2 \mu\text{m}$). Each pore initially contains one bubble as multiple small bubbles in the same pore will quickly fuse into one (rationalized in Supporting Information S1), and the average bubble volume \bar{V}_0 is $3.78 \times 10^{-1} \mu\text{m}^3$, which is set to be smaller than the volume of the largest inscribed sphere in the pore, V_{ins} , which is $4.18 \mu\text{m}^3$. The latter corresponds to the minimum curvature a bubble can assume in a pore. Detailed parameters of the simulation are chosen to be typical of geologic CO_2 sequestration operations and are listed in the Supporting Information S1.

Figure 2a shows the evolution of every bubble's volume in this demonstration, where we can identify two ripening stages:

- *Coarsening stage.* It happens at early time. In the coarsening stage, small bubbles dissolve and absorb into large bubbles. The ripening direction is the same as classical LSW ripening in bulk fluid, as the bubbles are still spherical and larger bubbles are of lower pressure. However, Figure 2b shows that the $r_c^3 - t$ scaling from LSW theory fails in this stage, and a much slower scaling of coarsening is observed. Because the driving

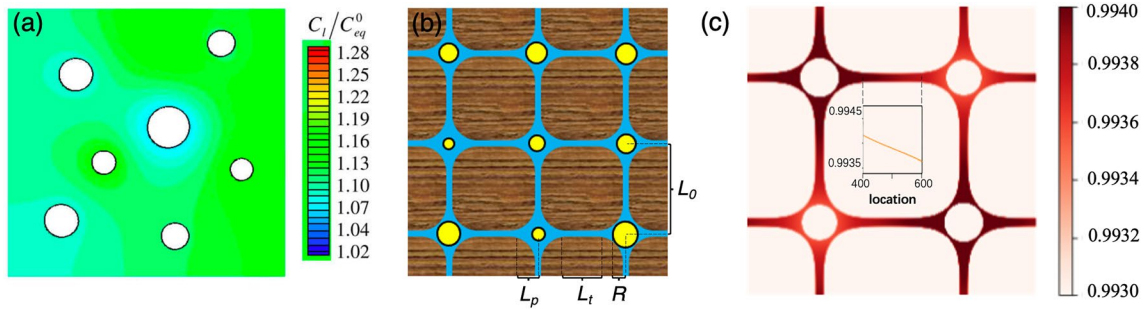


Figure 1. (a) Direct numerical simulation result of concentration field during bubble ripening in a bulk fluid in the absence of convection; copyright obtained from (Sun & Beckermann, 2010); (b) Schematic of bubbles in a porous medium, with geometric parameters annotated. Note that bubbles are confined in pore bodies, while they can exchange mass with neighboring pores through throats; (c) Concentration field during four bubble ripening in porous media using a phase-field method (Shimizu & Tanaka, 2017). Note that the concentration along the throat is approximately linear as shown in the inserted concentration profile along the throat, while concentration inside the pore body is relatively uniform.

force of ripening is the same as that in LSW theory, the deviation from LSW theory must be a result of mass transfer kinetics.

- *Anti-coarsening stage.* It happens at late times when coarsening stops so bubbles cease to disappear. In this stage, the ripening direction reverses until they attain identical capillary pressure. The transition from coarsening to anti-coarsening is attributed to the non-monotonicity in the $P_c - V_b$ relation of bubbles. Anti-coarsening kinetics have been well-studied recently (de Chalendar et al., 2018; K. Xu et al., 2017).

It is worth noting that, almost all changes associated with interfacial free energy and spatial redistribution of bubbles occur during the coarsening stage, as shown in Figure 2c. By contrast, changes during the anti-coarsening stage are negligible, although it takes much longer time and gets much attention in recent years (de Chalendar et al., 2018; Xu et al., 2017). It is therefore reasonable to approximate the equilibrium state of a bubble population as that immediately preceding the anti-coarsening stage. In other words, it is the kinetics of the coarsening stage that determines the equilibrium configuration of bubbles in a porous medium—but classical LSW theory cannot predict this coarsening process.

3. Theory of Coarsening Kinetics in Porous Media

3.1. Assumptions

Here, we focus on a homogenous porous medium for simplicity and comparison with the above numerical modeling. All pores are of identical size, shape, and connectivity to neighbors. We assume bubbles are perfectly non-wetting. The initial condition is assumed to consist of bubbles immediately after nucleation, which implies there are no bubbles that span multiple pores. All bubbles thus share identical $P_c - V_b$ relation. In addition, we

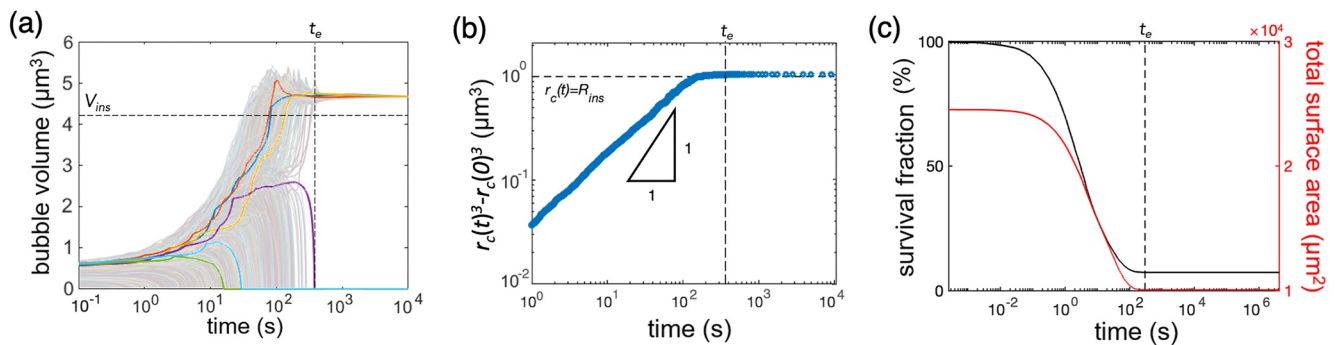


Figure 2. Ripening kinetics of 40,000 bubbles over time in the demonstrative case. Bubbles are trapped inside a 200×200 lattice pore network. (a) The evolution of every bubble's volume over time. (b) Comparison between simulation results of r_c evolution and the $r_c^3 \sim t$ scaling from LSW theory. Note the evolution of r_c overtime is sublinear, that is, is slower than LSW theory. (c) Evolution of the fraction of bubble count over time. Overlaid is the total interfacial surface area (proportional to surface free energy) over time. For all three plots, dramatic change of mode emerges at t_c as represented by the vertical dashed lines.

assume that throat width is much narrower than the pore body so the major mass transfer resistance is along throats; otherwise, if the grain is small enough compared to the throat (which is not realistic in subsurface environment), the kinetics will be regressed to LSW theory. We assume the conservation of gas saturation, S , the ratio of total bubble volume over total void space volume. This assumption is valid when P_c is much smaller than the ambient pressure that holds for most subsurface scenarios (Bauget & Lenormand, 2010). We leave the impacts of heterogeneity, wettability, and multi-pore spanning bubbles to future work.

3.2. Single Bubble Evolution

Before resolving the collective evolution of the bubble population during the coarsening stage, we first revisit the evolution kinetics of a single bubble in a porous medium. For a single bubble exchanging mass with its surrounding fluid, two length scales are relevant:

- The length scale associated with the mass transfer between the bubble and a “mean field” or infinitely far environment, L_{c_env} . In a bulk fluid, this is proportional to the bubble radius, but in a porous medium, it is proportional to the pore size (i.e., $L_{c_env} \propto L_0$) as pore-throat structure “quantizes” the space, as we discussed in introduction.
- The length scale associated with the mass transfer between the bubble and its neighboring bubbles, L_{c_int} . This depends on the average bubble-to-bubble distance, which can be expressed at fixed total bubble volume as $L_{c_int} \propto R_c^{3/d}$ where R_c is the characteristic radius of the bubble population and d is the problem dimension (two for 2D pore-network, and three for 3D pore-network).

The evolution kinetics of a single bubble is determined by the characteristic mass transfer distance $L_c = \min[L_{c_env}; L_{c_int}]$. That is, when bubbles are densely packed, bubble-bubble interactions dominate, but when bubbles are sparsely packed, they can be approximated as exchanging mass with an infinite mean field. In both cases, the evolution of the bubble’s volume is described by:

$$\frac{dV_b}{dt} = -\frac{C^*}{L_c} \left(\frac{1}{R_c} - \frac{1}{R} \right) \quad (2)$$

where C^* is a constant that incorporates the effects of solubility, surface tension, Henry’s constant, and pore geometry. Explicit formulas for both L_c and C^* are derived in the Supporting Information S1.

3.3. Bubble Population Evolution

Substituting Equation (2) into the total bubble volume conservation, $\sum_i \frac{dV_{b,i}}{dt} = 0$, yields $R_c = N / \sum_i (1/R_i)$. Notice that R_c is the harmonic mean of bubble radii, not equal to r_c from LSW theory which is the arithmetic mean (Bray, 2002).

The next step is to write down a probability distribution function for the bubble radii, $n(R, t)$, defined as the derivative of the number density of bubbles with respect to R . We expect a self-similar expression for $n(R, t)$, similar to the classical LSW theory (Bray, 2002). We thus decompose $n(R, t)$ into a time-dependent term and a time-independent term as $n(R, t) = f(x) \cdot R_c^{-d}(t)$, where $x = R/R_c$ and $f(x)$ is the probability density function of x . We substitute this into the continuity equation for $n(R, t)$:

$$\frac{\partial n(R, t)}{\partial t} + \frac{\partial}{\partial R} (n(R, t)v(R)) = 0 \quad (3)$$

to obtain:

$$L_c \dot{R}_c R_c^3 (x f' + 4 f') = C \cdot [f'(x^{-2} - x^{-3}) + f(-2x^{-3} + 3x^{-4})] \quad (4)$$

where $v(R) = \frac{dR}{dt} = \frac{C}{L_c R_c^2} \cdot \left(\frac{1}{R_c R^2} - \frac{1}{R^3} \right)$ according to Equation (2).

Note that $f(x)$ is not a function of time. Given that R_c and $f(x)$ are independent, we can write $L_c \dot{R}_c R_c^3 = C_1 C$ where $C_1 = 27/256$. After imposing the constraint that $\int_0^\infty f(x) = 1$, we arrive at the relative bubble-size distribution:

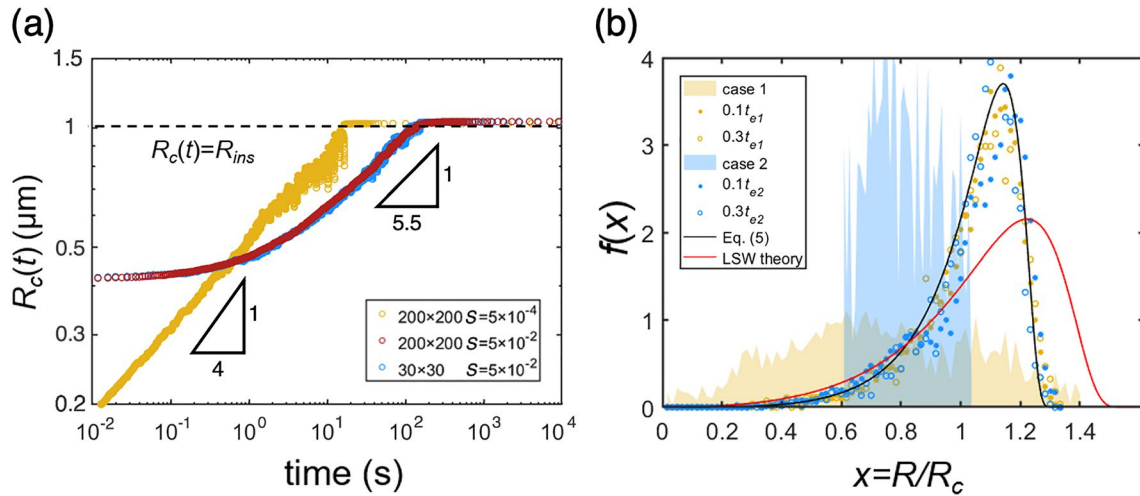


Figure 3. Comparison between theory and numerical simulations. (a) The evolution of the bubbles' harmonic mean radius with time, for three different cases: bubbles in a 200×200 matrix with gas saturation $S = 5 \times 10^{-4}$ (yellow circles); bubbles in a 200×200 matrix with gas saturation $S = 5 \times 10^{-2}$ (red circles); bubbles in a 30×30 matrix with gas saturation $S = 5 \times 10^{-2}$ (blue circles). Note that the scaling matches well with the theoretical prediction, independent of model size. (b) Comparison between the analytical solution of $f(x)$ and numerical simulation results at time $0, 0.1 t_e, 0.3 t_e$. Note that $f(x)$ is independent of initial bubble size distributions (drawn), Equation (5) well matches the simulation, and LSW theory fails.

$$f(x) = 9190x^3(4 - 3x)^{-\frac{19}{6}}(3x^2 + 8x + 16)^{-\frac{23}{12}} \exp \left[\frac{2}{3x - 4} - \frac{\sqrt{2}}{12} \tan^{-1} \left(\frac{3x + 4}{4\sqrt{2}} \right) \right] \quad (5)$$

Surprisingly, $f(x)$ does not depend on either L_c or d . The evolution kinetics for R_c can now be derived by substituting Equation (5) into Equation (4), provided an expression for L_c is available. For a densely packed bubble population, $L_c = L_{c_int} \propto R_c^{3/d}$, and so $L_c \dot{R}_c R_c^3 = C_1 C$ and $R_c^{4+3/d} \sim t$. For a sparsely packed bubble population, $L_c = L_{c_env} \propto L_0$, and so $L_c \dot{R}_c R_c^3 = C_1 C$ and $R_c^4 \sim t$. Exact expressions for these two scenarios can be derived respectively:

$$R_c^{\frac{3}{d}+4}(t) - R_c^{\frac{3}{d}+4}(0) = \frac{27 D_m x_0 \sigma A_t V_{mb}}{512 \pi K_{px} L_t V_{mw}} \left(\frac{3}{d} + 4 \right) \left(\frac{3 \bar{V}_0}{4a\pi} \right)^{\frac{1}{d}} t \quad (6)$$

for densely packed bubbles, and

$$R_c^4(t) - R_c^4(0) = \frac{27 D_m x_0 \sigma A_t M_b V_{mw} t}{64 \pi K_{px} L_p M_w V_{mb}} \quad (7)$$

for sparsely packed bubbles. Here, D_m is the Fickian diffusion coefficient, K_{px} Henry's constant, A_t the cross-sectional area of each throat, x_0 is the saturated mole fraction of the bubble component dissolved in the surrounding liquid phase, V_{mb} the molar volume of the non-wetting phase, V_{mw} the molar volume of the wetting phase, M_b is the molecular weight of the non-wetting phase, and M_w the molecular weight of the wetting phase. The details of the above derivation are given in Supporting Information S1.

We next validate the above derivation using PNM simulations (Y. Mehmani & Xu, 2022a, 2022b). If we set the initial mean bubble volume to $\bar{V}_0 \ll V_{ins}$, the spatial distribution of bubbles would become more and more sparse as they coarsen. We would therefore expect $R_c^4 \sim t$. But if \bar{V}_0 is relatively large (but the bubble is still spherical), bubbles transfer mass primarily with neighboring bubbles, and an $R_c^{4+3/d} \sim t$ scaling is expected. We note that in our simulations, the pore-network is 2D so $d = 2$, so $4 + 3/d = 5.5$. Figure 3a shows that our theoretical prediction is in excellent agreement with PNM simulations. Figure 3b compares simulated bubble-size distributions at different times with different initial distributions, against the analytical solution in Equation (5). Here too, the agreement is very good regardless of the initial distribution and \bar{V}_0 . Note the predictions are also very different from that of LSW theory.

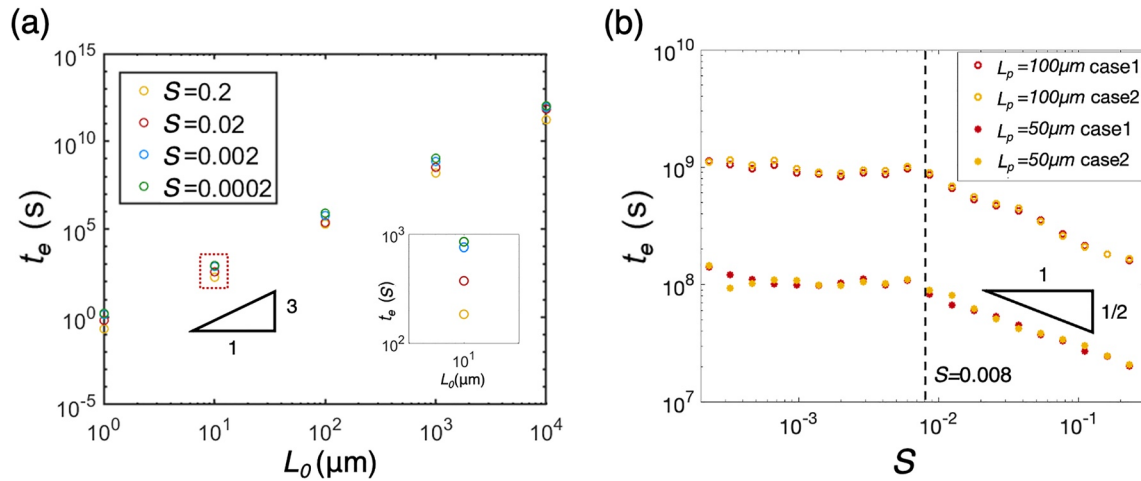


Figure 4. (a) The numerical time required for bubble populations to reach thermodynamic stability when changing the pore-network lattice L_0 from 1 μm to 10 mm and changing the gas saturation S from 0.0002 to 0.2. (b) The numerical time required for bubble populations to reach thermodynamic stability when changing the gas saturation S from 0.0002 to 0.2 with $L_p = 100 \mu\text{m}$ and $L_p = 50 \mu\text{m}$ (see Supporting Information S1 for data of more L_p values).

4. Equilibrium Time and Its Practical Implication

We note that the coarsening toward quasi-equilibrium in porous media is local, as both Equations (6) and (7) contain no variable correlated to the problem size. This claim is supported by the simulation results that R_c evolution in a 200×200 lattice pore network overlaps with that in a 30×30 lattice pore network (Figure 3a). It is distinct from the anti-coarsening stage in porous media that kinetics is strongly correlated to the scale of the system (Li et al., 2021). As a result, the time for the system to reach thermodynamic quasi-equilibrium (transition from coarsening to anti-coarsening), t_e , is local and determined only by pore-scale geometry and fluid properties.

We therefore define t_e the moment of $R_c(t_e) = R_{\text{ins}}$, which is the radius of a spherical bubble with volume V_{ins} , into Equations (6) and (7). For both densely and sparsely distributed bubbles, it can be estimated that:

$$t_e = FGD_s t_d \quad (8)$$

where F is a scale-free coefficient that only depends on fluids' properties and the pore-throat shape (not size), G is a function of dimension and gas saturation S . Easy to derive that $F = \left(\frac{R_{\text{ins}}^2}{A_t}\right) \left(\frac{R_{\text{ins}}}{L_t}\right) \left(\frac{V_{\text{mw}}}{V_{\text{mb}}}\right)$ for both limits, while

$G = \frac{512\pi}{(108 + \frac{81}{d})x_0} \left(\frac{V_{\text{pore}}}{V_{\text{ins}}}\right)^{\frac{1}{d}} S^{-\frac{1}{d}}$ for densely distributed bubbles and $G = \frac{64\pi}{27} \left(\frac{L_p}{L_t}\right) \left(\frac{M_w}{M_b}\right) \left(\frac{V_{\text{mb}}}{V_{\text{mw}}}\right)^2$ for sparsely distributed bubbles. $D_s = R_{\text{ins}} K_{\text{px}} / \sigma \propto L_0$ is minimum extra solubility due to capillary pressure, $t_d = L_t^2 / D_m \propto L_0^2$ is characteristic diffusion time between two neighboring pores.

According to the above analytical derivation or equilibrium time, we can infer that, (a) with a fixed porous shape and fluid system (fixed F and G), $t_e \propto L_0^3$; and (b) with fixed F , D_s , and t_d , t_e is independent of S at the sparse limit and is negatively correlated to S as $t_e \propto S^{-1/d}$ at the dense limit. We then conduct numerical simulations with different L_0 (from 0.1 μm to 10 mm) and gas saturation S (from 0.0002 to 0.2) to validate the above analytical expression and discussion of equilibrium time. As shown in Figures 4a and 4b, the numerically measured t_e well matches our theoretical estimation for both dense and sparse cases.

5. Implications

5.1. Critical Saturation

The critical saturation, S_{crit} , for bubble population to transient from “dense” to “sparse” can be estimated by equating t_e in two scenarios. It yields:

$$S_{\text{crit}} = \left[\left(\frac{27}{108 + \frac{81}{d}} \right) \left(\frac{L_t}{L_p} \right) \left(\frac{V_{mw}^2 M_b}{V_{mb}^2 M_w} \right) \right]^d \left(\frac{V_{\text{pore}}}{V_{\text{ins}}} \right). \quad (9)$$

We note that this critical S is not relevant to exact pore size, but a function of dimension, pore shape, and fluid properties. In our demonstrative case, $S_{\text{crit}} = 0.008$, which is well supported by numerical simulation as shown in Figure 4b. For subsurface CO_2 -water system in a 3-D pore network, it is easy to conclude that bubbles in porous media should always be “dense” when gas saturation is of practical significance.

5.2. Equilibrium Time

The value of t_e is highly sensitive to pore size as $t_e \propto L_0^3$, which could fall in a very wide interval for different natural porous media, as presented in Figures 4a and 4b. For the demonstrative fluid system, t_e could be as short as milli-seconds when $L_0 = 1 \mu\text{m}$ (common for fine sandstone and shale (Zou et al., 2015)), and as long as 30 years when $L_0 = 1 \text{mm}$ (not rare in coarse limestone).

Comparison between t_e against the characteristic time of any other concerned physical process (Cugliandolo, 2010; Ngamsaad et al., 2010) determines whether the local thermodynamic equilibrium presumption is valid. When t_e is comparably short, bubbles can be considered as equilibria immediately when they are nucleated, which rationalizes recent experimental observation (Berg et al., 2020) that only non-spherical large bubbles are observed quickly after bubble nucleation in a rock sample. In contrast, if t_e is comparably large, the thermodynamic equilibrium of bubbles may be invalid.

5.3. Limitations

As a preliminary effort to theoretically identify the coarsening kinetics of bubbles in porous media, this work adopts highly ideal assumptions, such as uniform pore size and shape, completely non-wetting bubbles, and the absence of external field. These simplifications allow simple analytical solutions. Nevertheless, in further practical investigations relevant to bubble evolution in subsurface porous media, these simplifications should be removed. Specifically, theories for the ripening of large bubbles spanning multiple pores should be constructed in the future, based on some preliminary numerical results (Singh et al., 2022; Y. Mehmani & Xu, 2022a).

In addition, we believe future experimental work, including microfluidic experiments and X-ray tomography and image analysis (Berg et al., 2020; Bultreys et al., 2020; Spurin et al., 2020), would be very helpful in validating our theory and extending it in identifying bubble’s spatial distribution, especially in heterogeneous media.

6. Conclusion

We numerically demonstrate that bubbles in porous media coarsen toward thermodynamic equilibrium, but the $r_c^3 \sim t$ scaling from classical LSW theory fails to describe its kinetics. The failure of LSW theory in porous media is that the porous structure decouples the bubble size and its mass transfer length scale. This separation of scales results in two much slower coarsening kinetics, $R_c^{3/d+4} \sim t$ and $R_c^4 \sim t$, for densely and sparsely distributed bubble populations, respectively, with the former practically more important in subsurface environment. Theoretical solution for bubble coarsening and bubble size distribution perfectly matches the PNM simulations.

We define bubbles’ thermodynamic equilibrium time, t_e , as the end of coarsening stage, during which majority of energy dissipation completes. After t_e , the system’s pore occupancy and interfacial area are determined, which are crucial parameters in characterizing and predicting multiphase flow and transport in porous media (Armstrong et al., 2018). In addition, the magnitude of t_e may be as small as sub-seconds and as large as thousands of years in different typical subsurface porous media, so it is necessary to compare the kinetics of ripening against other processes of interest to examine the local capillary equilibrium assumption, in applications such as geologic CO_2 sequestration, oil and gas recovery, and groundwater systems.

More generally, this work reveals that mass transfer is fundamentally altered in porous media, by decoupling the mass transfer coefficient from details inside the pore body. Following recent findings that porous structure deforms the interface and thus modifies mass transfer driving force (Blunt, 2022; Ke Xu et al., 2019; K. Xu et al., 2017; Wang et al., 2021), we are now one step further toward finally understanding the evolution of multi-phase fluid systems in subsurface porous media.

Data Availability Statement

Parameters and derivations applied in this work are shown in Supporting Information S1. Information of numerical simulation is demonstrated in detail in our earlier publication (Y. Mehmani et al., 2014). Data presented in figures are publicly available through [zenodo.org](https://doi.org/10.5281/zenodo.6967314) (<https://doi.org/10.5281/zenodo.6967314>).

Acknowledgments

We gratefully acknowledge the financial support and funding provided by the National Key Research and Development Program of China under Grant 2021YFA0717200, by the National Natural Science Foundation of China under Grant 12172010, and by the CNPC Research Institute of Petroleum Exploration and Development for the project “Key Fluid Mechanisms of CO₂-EOR for Gu-Long Shale Oil Development.” Yashar Mehmani acknowledges the Department of Energy and Mineral Engineering (EME) and the College of Earth and Mineral Sciences (EMS) for providing the funds for this project. The authors thank Dr. Sally Benson for helpful discussions during AGU2019 conference.

References

- Anton, L., & Hilfer, R. (1999). Trapping and mobilization of residual fluid during capillary desaturation in porous media. *Physical Review E, Statistical Physics, Plasmas, Fluids, and Related Interdisciplinary Topics*, 59(6), 6819–6823. <https://doi.org/10.1103/physreve.59.6819>
- Armstrong, R. T., McClure, J. E., Robins, V., Liu, Z., Arms, C. H., Schlüter, S., & Berg, S. (2018). Porous media characterization using minkowski functionals: Theories, applications and future directions. *Transport in Porous Media*, 130(1), 305–335. <https://doi.org/10.1007/s11242-018-1201-4>
- Bauget, F., & Lenormand, R. (2010). Mechanisms of bubble formation by pressure decline in porous media: A critical review. *SOCAR Proceedings*, 2010(3).
- Bear, J. (1996). *Modeling phenomena of flow and transport in porous media* (Vol. 31). Springer International Publishing.
- Berg, S., Gao, Y., Georgiadis, A., Brussee, N., Coorn, A., Van derLinde, H., et al. (2020). Determination of critical gas saturation by micro-CT. *Petrophysics. The SPWLA Journal of Formation Evaluation and Reservoir Description*, 61(2), 133–150. <https://doi.org/10.30632/pjv61n2-2020a1>
- Blunt, M. J. (2022). Ostwald ripening and gravitational equilibrium: Implications for long-term subsurface gas storage. *Physical Review E*, 106(4), 045103. <https://doi.org/10.1103/physreve.106.045103>
- Bray, A. J. (2002). Theory of phase-ordering kinetics. *Advances in Physics*, 51(2), 481–587. <https://doi.org/10.1080/00018730110117433>
- Bultreys, T., Singh, K., Raeni, A. Q., Ruspini, L. C., Øren, P. E., Berg, S., et al. (2020). Verifying pore network models of imbibition in rocks using time-resolved synchrotron imaging. *Water Resources Research*, 56(6). <https://doi.org/10.1029/2019wr026587>
- Cugliandolo, L. F. (2010). Topics in coarsening phenomena. *Physica A: Statistical Mechanics and its Applications*, 389(20), 4360–4373. <https://doi.org/10.1016/j.physa.2009.12.036>
- Danov, K. D., Valkovska, D. S., & Kralchevsky, P. A. (2003). Hydrodynamic instability and coalescence in trains of emulsion drops or gas bubbles moving through a narrow capillary. *Journal of Colloid and Interface Science*, 267(1), 243–258. [https://doi.org/10.1016/s0021-9797\(03\)00596-4](https://doi.org/10.1016/s0021-9797(03)00596-4)
- de Chalendar, J. A., Garing, C., & Benson, S. M. (2018). Pore-scale modelling of Ostwald ripening. *Journal of Fluid Mechanics*, 835, 363–392. <https://doi.org/10.1017/jfm.2017.720>
- Ehlers, W., & Häberle, K. (2016). Interfacial mass transfer during gas–liquid phase change in deformable porous media with heat transfer. *Transport in Porous Media*, 114(2), 525–556. <https://doi.org/10.1007/s11242-016-0674-2>
- Fu, X., Cueto-Felgueroso, L., & Juanes, R. (2013). Pattern formation and coarsening dynamics in three-dimensional convective mixing in porous media. *Philosophical Transactions of the Royal Society A: Mathematical, Physical and Engineering Sciences*, 371(2004), 20120355. <https://doi.org/10.1098/rsta.2012.0355>
- Gao, Y., Georgiadis, A., Brussee, N., Coorn, A., vander Linde, H., Dieterich, J., et al. (2021). Capillarity and phase-mobility of a hydrocarbon gas–liquid system. *Oil & Gas Science and Technology—Revue d'IFP Energies nouvelles*, 76, 43. <https://doi.org/10.2516/ogst/2021025>
- Geistlinger, H., Ataei-Dadavi, I., Mohammadian, S., & Vogel, H. J. (2015). The impact of pore structure and surface roughness on capillary trapping for 2-D and 3-D porous media: Comparison with percolation theory. *Water Resources Research*, 51(11), 9094–9111. <https://doi.org/10.1002/2015wr017852>
- Holocher, J., Peeters, F., Aeschbach-Hertig, W., Kinzelbach, W., & Kipfer, R. (2003). Kinetic model of gas bubble dissolution in groundwater and its implications for the dissolved gas composition. *Environmental Science & Technology*, 37(7), 1337–1343. <https://doi.org/10.1021/es025712z>
- Huppert, H. E., & Neufeld, J. A. (2014). The fluid mechanics of carbon dioxide sequestration. *Annual Review of Fluid Mechanics*, 46(1), 255–272. <https://doi.org/10.1146/annurev-fluid-011212-140627>
- Joewondo, N., Garbin, V., & Pini, R.-M. (2021). *Direct imaging of bubble ripening in two-dimensional porous media micromodels*. Paper presented at the Proceedings of the 15th Greenhouse Gas Control Technologies Conference.
- Juanes, R., Spiteri, E. J., Orr, F. M., & Blunt, M. J. (2006). Impact of relative permeability hysteresis on geological CO₂ storage. *Water Resources Research*, 42(12). <https://doi.org/10.1029/2005wr004806>
- Lay, J.-J., Miyahara, T., & Noike, T. (1996). Methane release rate and methanogenic bacterial populations in lake sediments. *Water Research*, 30(4), 901–908. [https://doi.org/10.1016/0043-1354\(95\)00254-5](https://doi.org/10.1016/0043-1354(95)00254-5)
- Lifshitz, I. M., & Slyozov, V. V. (1961). The kinetics of precipitation from supersaturated solid solutions. *Journal of Physics and Chemistry of Solids*, 19(1–2), 35–50. [https://doi.org/10.1016/0022-3697\(61\)90054-3](https://doi.org/10.1016/0022-3697(61)90054-3)
- Li, Y., Garing, C., & Benson, S. M. (2020). A continuum-scale representation of Ostwald ripening in heterogeneous porous media. *Journal of Fluid Mechanics*, 889, A14. <https://doi.org/10.1017/jfm.2020.53>
- Li, Y., Orr, F. M., & Benson, S. M. (2021). Long-term redistribution of residual gas due to non-convective transport in the aqueous phase. *Transport in Porous Media*, 141(1), 231–253. <https://doi.org/10.1007/s11242-021-01722-y>
- Lyu, X., Voskov, D., & Rossen, W. R. (2021). Numerical investigations of foam-assisted CO₂ storage in saline aquifers. *International Journal of Greenhouse Gas Control*, 108, 103314. <https://doi.org/10.1016/j.ijggc.2021.103314>
- Mehmani, A., Kelly, S., Torres-Verdin, C., & Balhoff, M. (2019). Capillary trapping following imbibition in porous media: Microfluidic quantification of the impact of pore-scale surface roughness. *Water Resources Research*, 55(11), 9905–9925. <https://doi.org/10.1029/2019wr025170>

- Mehmani, Y., Oostrom, M., & Balhoff, M. T. (2014). A streamline splitting pore-network approach for computationally inexpensive and accurate simulation of transport in porous media. *Water Resources Research*, 50(3), 2488–2517. <https://doi.org/10.1002/2013wr014984>
- Mehmani, Y., & Xu, K. (2022a). Capillary equilibration of trapped ganglia in porous media: A pore-network modeling approach. *Advances in Water Resources*, 166, 104223. <https://doi.org/10.1016/j.advwatres.2022.104223>
- Mehmani, Y., & Xu, K. (2022b). Pore-network modeling of Ostwald ripening in porous media: How do trapped bubbles equilibrate? *Journal of Computational Physics*, 457, 111041. <https://doi.org/10.1016/j.jcp.2022.111041>
- Ngamsaad, W., Yojina, J., & Triampo, W. (2010). Theoretical studies of phase-separation kinetics in a Brinkman porous medium. *Journal of Physics A: Mathematical and Theoretical*, 43(20), 202001. <https://doi.org/10.1088/1751-8113/43/20/202001>
- Ozgumus, T., & Mobedi, M. (2015). Effect of pore to throat size ratio on interfacial heat transfer coefficient of porous media. *Journal of Heat Transfer*, 137(1). <https://doi.org/10.1115/1.4028764>
- Rogers, T. M., & Desai, R. C. (1989). Numerical study of late-stage coarsening for off-critical quenches in the Cahn-Hilliard equation of phase separation. *Physical Review B*, 39(16), 11956–11964. <https://doi.org/10.1103/physrevb.39.11956>
- Schmelzer, J., Möller, J., & Slezov, V. V. (1995). Ostwald ripening in porous materials: The case of arbitrary pore size distributions. *Journal of Physics and Chemistry of Solids*, 56(8), 1013–1022. [https://doi.org/10.1016/0022-3697\(95\)00021-6](https://doi.org/10.1016/0022-3697(95)00021-6)
- Shimizu, R., & Tanaka, H. (2017). Impact of complex topology of porous media on phase separation of binary mixtures. *Science Advances*, 3(12), eaap9570. <https://doi.org/10.1126/sciadv.aap9570>
- Singh, D., Friis, H. A., Jettstuen, E., & Helland, J. O. (2022). A level set approach to Ostwald ripening of trapped gas bubbles in porous media. *Transport in Porous Media*.
- Slezov, V. V., Schmelzer, J., & Möller, J. (1993). Ostwald ripening in porous materials. *Journal of Crystal Growth*, 132(3–4), 419–426. [https://doi.org/10.1016/0022-0248\(93\)90067-7](https://doi.org/10.1016/0022-0248(93)90067-7)
- Spurin, C., Bultreys, T., Rücker, M., Garfi, G., Schlepütz, C. M., Novak, V., et al. (2020). Real-time imaging reveals distinct pore-scale dynamics during transient and equilibrium subsurface multiphase flow. *Water Resources Research*, 56(12). <https://doi.org/10.1029/2020wr028287>
- Sun, Y., & Beckermann, C. (2010). Phase-field modeling of bubble growth and flow in a Hele–Shaw cell. *International Journal of Heat and Mass Transfer*, 53(15–16), 2969–2978. <https://doi.org/10.1016/j.ijheatmasstransfer.2010.03.036>
- Voorhees, P. W. (1985). The theory of Ostwald ripening. *Journal of Statistical Physics*, 38(1), 231–252. <https://doi.org/10.1007/bf01017860>
- Wagner, C. (1961). Theorie der alterung von niederschlägen durch umlösen (Ostwald-reifung). *Zeitschrift für Elektrochemie, Berichte der Bunsengesellschaft für physikalische Chemie*, 65(7–8), 581–591. <https://doi.org/10.1002/bbpc.19610650704>
- Wang, C., Mehmani, Y., & Xu, K. (2021). Capillary equilibrium of bubbles in porous media. *Proceedings of the National Academy of Sciences*, 118(17), e2024069118. <https://doi.org/10.1073/pnas.2024069118>
- Xu, K., Bonnacaze, R., & Balhoff, M. (2017). Egalitarianism among bubbles in porous media: An Ostwald ripening derived anticoarsening phenomenon. *Physical Review Letters*, 119(26), 264502. <https://doi.org/10.1103/physrevlett.119.264502>
- Xu, K., Mehmani, Y., Shang, L., & Xiong, Q. (2019). Gravity-induced bubble ripening in porous media and its impact on capillary trapping stability. *Geophysical Research Letters*, 46(23), 13804–13813. <https://doi.org/10.1029/2019gl085175>
- Yao, J. H., Elder, K. R., Guo, H., & Grant, M. (1993). Theory and simulation of Ostwald ripening. *Physical Review B*, 47(21), 14110–14125. <https://doi.org/10.1103/physrevb.47.14110>
- Yortsos, Y. C., & Stubos, A. K. (2001). Phase change in porous media. *Current Opinion in Colloid & Interface Science*, 6(3), 208–216. [https://doi.org/10.1016/s1359-0294\(01\)00085-1](https://doi.org/10.1016/s1359-0294(01)00085-1)
- Zou, C., Jin, X., Zhu, R., Gong, G., Sun, L., Dai, J., et al. (2015). Do shale pore throats have a threshold diameter for oil storage? *Scientific Reports*, 5(1), 13619. <https://doi.org/10.1038/srep13619>